

Enhancing Contrast in Optical Imaging of Cancer tissues and Study the Spectral Properties of Methylene Blue

S. Malik ^{a,b,c}, H. Ullah ^{a*}, F. Andleeb ^{a,b}, Z. Batool ^a, A. Nazir ^a, G. Gilanie ^e, M. Nisa ^b, A. Rashid ^d

^aBiophotonics Imaging Techniques Laboratory, Department of Physics, The Islamia University of Bahawalpur, Pakistan.

^bDepartment of Physics, Govt Sadiq College women University, Bahawalpur, Pakistan.

^cAdvanced Biophotonics Laboratory, University of Massachusetts Lowell, Lowell MA, USA.

^dUniversity College of Engineering and Technology, The Islamia University of Bahawalpur.

^eDepartment of Computer Science, Faculty of Computing, The Islamia University of Bahawalpur, Bahawalpur, Pakistan.

*Corresponding Author, E-mail: hafeezullah@iub.edu.pk, phone: +92 344 7181418

Received: 15-01-2021 Accepted: 04-08-2021

Published: 17-09-2021

ABSTRACT

The primary focus of this experiment was to study of optical imaging of malignant and normal tissues (skin and breast) and to observe the spectral properties of Methylene Blue and its potential use as a cancer biomarker in the diagnosis of breast cancer tissues. We present the optical imaging of skin tissues by different techniques, including reflectance, fluorescence and polarization imaging for early detection of skin cancer. We collected the reflectance images of skin between 410 nm and 630 nm. We confirmed that a high concentration of MB occurs in cancer cells due to its increased accumulation in mitochondria of cancer cells. The breast tissues stained with MB were imaged with a high-resolution microscope. Imaging of breast cancer shows highly significant differences between cancer and normal cells using MB concentrations as low as 0.05 and 0.01 mg/ml. We also observed the fluorescence polarization and absorption and fluorescence emission spectrum of MB dissolved in solutions of saline and glycerol by using different solutions of methylene blue dye.

Keywords: Optical imaging; wide field imaging; skin tissue; Breast Cancer; Methylene Blue; Microscopy

Mejora del contraste en la obtención de imágenes ópticas de tejidos cancerosos y estudio de las propiedades espectrales del azul de metileno

RESUMEN

El objetivo principal de este experimento fue estudiar imágenes ópticas de tejidos malignos y normales (piel y mama) y observar las propiedades espectrales del azul de metileno y su uso potencial como biomarcador de cáncer en el diagnóstico de tejidos de cáncer de mama. Presentamos la imagen óptica de los tejidos de la piel mediante diferentes técnicas, que incluyen imágenes de reflectancia, fluorescencia y polarización para la detección precoz del cáncer de piel. Recolectamos las imágenes de reflectancia de piel entre 410 nm y 630 nm. Confirmamos que se produce una alta concentración de MB en las células cancerosas debido a su mayor acumulación en las mitocondrias de las células cancerosas. Se tomaron imágenes de los tejidos mamarios teñidos con MB con un microscopio de alta resolución. Las imágenes del cáncer de mama muestran diferencias muy significativas entre el cáncer y las células normales utilizando concentraciones de MB tan bajas como 0,05 y 0,01 mg / ml. También observamos la polarización de fluorescencia y el espectro de absorción y emisión de fluorescencia de MB disuelto en soluciones de solución salina y glicerol mediante el uso de diferentes soluciones de colorante azul de metileno.

Palabras claves: Imágenes ópticas; imágenes de campo amplio; tejido de la piel; Cáncer de mama; Azul de metileno; Microscopía

INTRODUCTION

Breast cancer is the most common carcinoma diagnosed in women and the second leading cause of death related to women [1]. Every year, 3.3 million women are affected with breast cancer in the US. Many factors contribute to development of breast cancer such as oestrogens [2].

Early detection of breast cancer can effectively reduce the subsequent mortality and morbidity [3,4]. Survival rate have increased due to advancement in screening and imaging techniques [5,6]. Rapid and accurate determination of cancers through imaging included near infrared spectroscopy, wide field imaging and multimodal

confocal microscopy [7]. Wide-field polarization imaging allows for a rapid macroscopic overview of the entire surface area of the tissue specimen [8]. Our group has proven that Methylene blue is a quantitative biomarker for the detection of breast cancer [9-11]. Skin malignancies are very common in USA [12] and every year, millions of people suffered from skin carcinoma, affecting millions worldwide. Skin cancer is generally classified as malignant melanoma and non-melanoma skin cancer (NMSC). We employed a linearly polarized monochromatic light source and a wide-field CCD camera for fluorescence polarization imaging of the nonmelanoma cancers stained with MB [13-16]. A combination of the large field of view and lateral resolution enables rapid investigation of large surfaces, thus examining tumor margin delineation [17]. Fluorescence polarization (Fpol) relies on the phenomenon that fluorescence molecules after excitation by linearly polarized light will emit plane-polarized light. This mechanism is based on the lifetime of the fluorophore being considered, In addition, it gives steady-state observations of cell diffusion, binding constants, the kinetics of reactions, and a wide range of mechanisms, in time-resolved measurements [18,19]. Contrary to fluorescence intensity, Fpol is independent on the concentration of the fluorophore, but quantum yield depends upon binding of fluorophore with macromolecule and size and molecular weight of molecules [20,21]. This fluorescence activity has been illustrated in a Jablonski energy diagram (figure 1).

Co-polarization describes Electromagnetic (EM) waves that have parallel polarization states. Cross-polarization describes EM waves that have perpendicular polarization states [22,23].

$$P = \frac{I_{fco} + G \times I_{fcross}}{I_{fco} - G \times I_{fcross}}$$

Figure 2 described the co and cross-polarization. After electron comes back to ground state, a fluorescent photon with lower energy as compared to the excitation light is emitted.

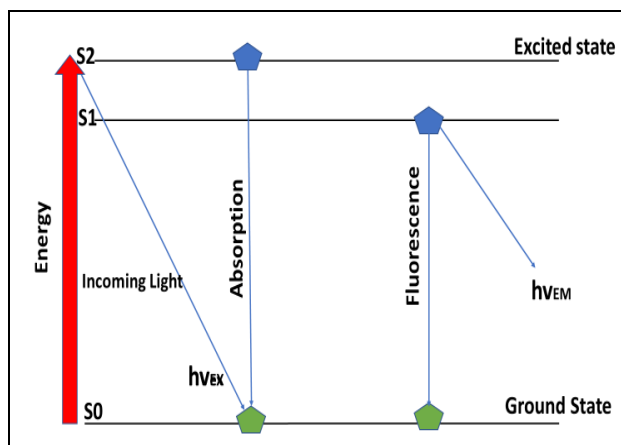


Fig. 1. The energy scale is represented by a red bar. S₀ is the ground state; S₁ and S₂ are the higher energy states.

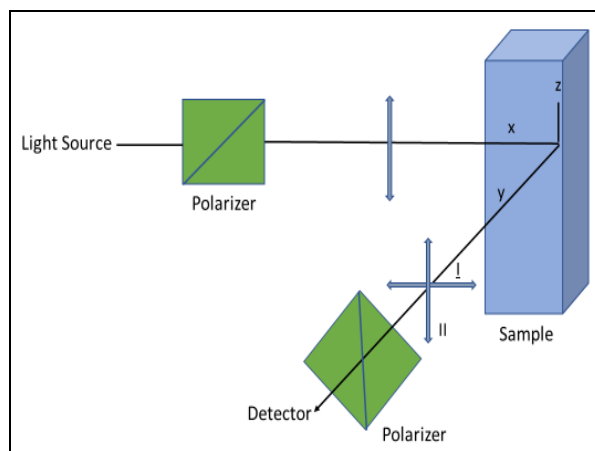


Fig. 2. Schematic drawing for the measurement of fluorescence polarization process describing co-polarization and cross-polarization.

Methylene blue is a fluorescent dye, which is FDA approved for human use. It shows promising applications in biophysics and used as medicine as well as dye. MB dye demonstrated a high degree of localization with the nucleus of cancer cells as compared to normal cells. Moreover, approximately 15% of cell volume is composed of mitochondria and enhanced accumulation of MB in these cell components shows a high value of fluorescence on the basis of which cancer cells can be diagnosed [24]. In this experiment we used PBS saline and Glycerol to obtain different concentrations of solutions.

MATERIALS AND METHODS

Sample preparation and handling

All experiments were performed at the Advanced Biophotonics laboratory. Discarded skin samples were acquired following surgery at the Department of Dermatology at Massachusetts General Hospital (MGH), Boston, and delivered to UMass Lowell (UML) Advanced Bio-photonics Laboratory for advanced imaging.

For this study, a total of 8 slides from 8 patients from breast cancer excision biopsies were used. The experiments were performed according to the protocols approved by the Institutional Review Boards of the University of Massachusetts at Lowell and the University of Massachusetts Memorial Medical Center at Worcester. Fresh excess breast tissue was obtained following surgical resection of breast tumors at UMass Memorial Medical Center. The size of fresh tissue samples ranged from 20 mm to 150 mm and the thickness from 3 to 7 mm. Specimens were soaked in 0.05 mg/ml DPBS solution of MB for approximately 10 min and then rinsed in DPBS to remove excess dye. After imaging, the tissue was fixed in formalin and processed for H&E paraffin embedded histopathology. The slides were routinely prepared with the standard procedure consisting of formalin fixation and paraffin embedding of the tissue, followed by cutting of 3 - 5 μm thick sections and staining with H&E. The H&E slides were then imaged with the high-resolution microscope.

Wide-field Reflectance imaging device

A picture of the wide field reflectance and fluorescence imaging machine is shown in figure 3. A xenon arc lamp (Lambda LS, Sutter, Novato, CA) connected with a computer controlled bandpass filter wheel (Lambda LS, Sutter, Novato, CA) was employed as the illuminator of light, assembled with 18 narrow band-pass filters (FWHM = 10), reflectance co- and cross-polarized images were registered between 390 nm to 750 nm and full width at half maximum of 10 nm. A 0.5 \times 0.5 Rodenstock lens conjugated to a CCD camera (PCO Tech, Kelheim, Germany) was employed for image acquisition. Linearly polarizing filters (Meadowlark

Optics, Frederick, CO) were used in passage of the light. The system provided a field of view of 40 mm \times 40 mm, and lateral resolution of 12 μm . Less than 3 min were required for image acquisition. The calibration factor of the system G, which describes efficiency of detection of co- and cross-polarized components of light, was constant ($G = 0.98$) [22].

The histopathology slides were imaged under the light microscope (PrimoVert, Carl Zeiss Microscopy, Peabody, MA) equipped with 20X/0.3 NA PIANAPO objective lens (Zeiss, Oberkochen, Germany). Images were stitched together by using a MetaMorph imaging software (Molecular Devices, Sunnyvale, CA). For the spectral analysis, we used a commercial spectrometer (Lambda 1050 UV/VIS/NIR, Perkin Elmer, Waltham, MA) and fluorometer (fluoromax-4, Horiba Scientific, Irvine, CA). For making the 0.01 mg/mL saline solution of MB, we used Phosphate Buffered Saline 1X solution (PBS, Sigma Aldrich, Burlington, MA, USA). For the 0.01 mg/ml MB glycerol solution, we used 99% glycerol.

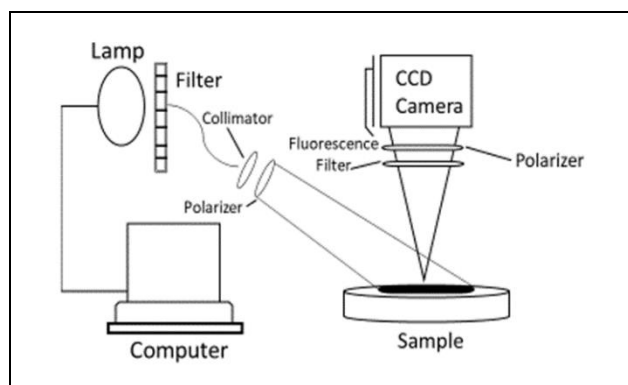


Fig. 3. Schematic diagram of the wide field-imaging device.

Methylene Blue Solutions

All mixing was carried out at atmospheric pressure using SCILOGEX MX-S agitation. Homogenous solutions of 0.01 mg/ml Methylene Blue (MB) in Phosphate-Buffered Saline (PBS) and 0.01 mg/ml MB in Glycerol were mixed. The MB-PBS solution was mixed for 1 min. MB is quickly mixed homogeneously in saline solution because of its low viscosity. For the MB-Glycerol solution,

homogenous mixing required approximately 20 - 30 min. As MB - Glycerol solution is more viscous than MB - PBS solution, longer mixing times were required to achieve uniform distribution of the dye throughout the solution.

RESULTS AND DISCUSSION

We registered skin reflectance images by using 0.5X lens with Photometrics CoolSnap camera. The co and cross, reflectance images of skin were acquired at the wavelengths of 410 nm, 430 nm, 570 nm and 630 nm. The field of view shown is 13.5 mm x 11 mm and the bar was 3 mm (figure 4-11).

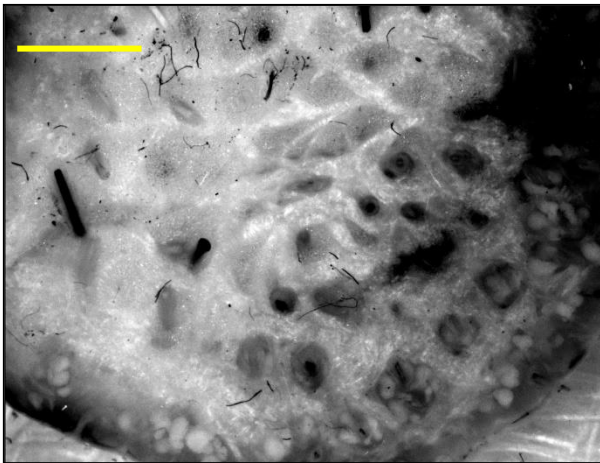


Fig. 4. Skin reflectance(cross-polarized) image at 410 nm wavelength. Exposure time was 1000 ms. Yellow bar: 3.4 mm.

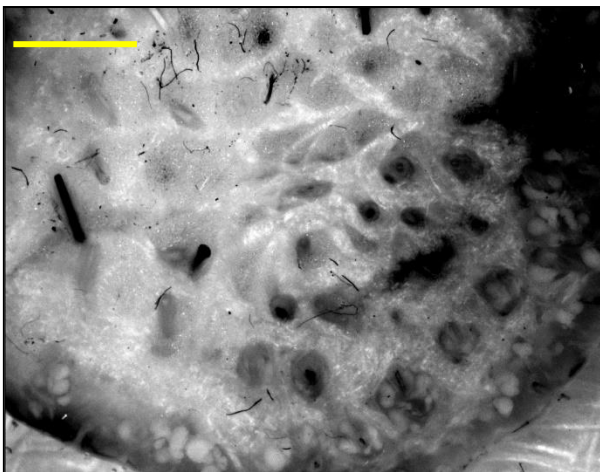


Fig. 5. Skin reflectance(cross-polarized) image at 430 nm wavelength. Exposure time was 500 ms. Yellow bar: 3.4 mm.

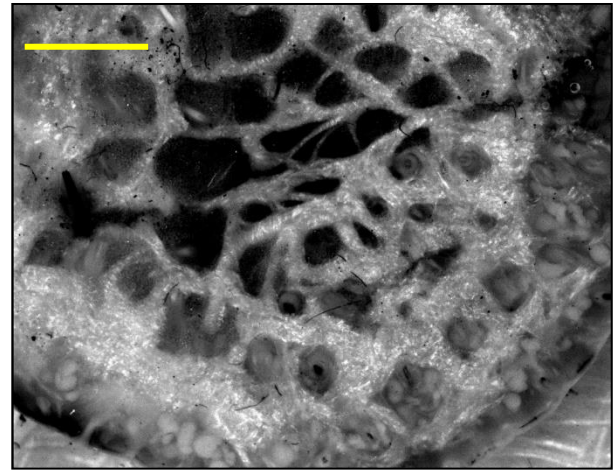


Fig. 6. Skin reflectance(co-polarized) image at 570 nm wavelength. Exposure time was 250 ms. Yellow bar: 3.4 mm.

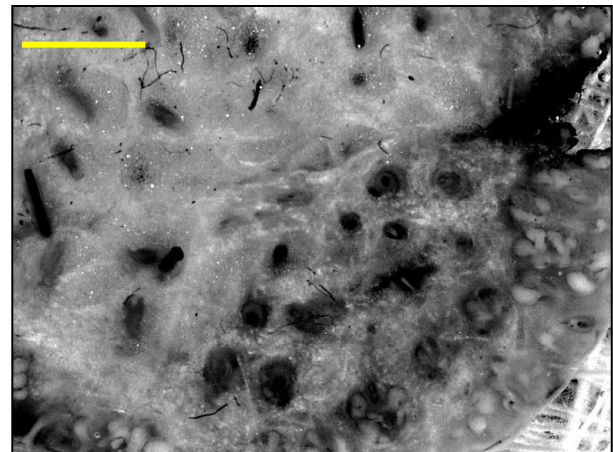


Fig.7. Skin reflectance(co-polarized) image at 630 nm wavelength. Exposure time was 330 ms. Yellow bar: 3.4 mm.

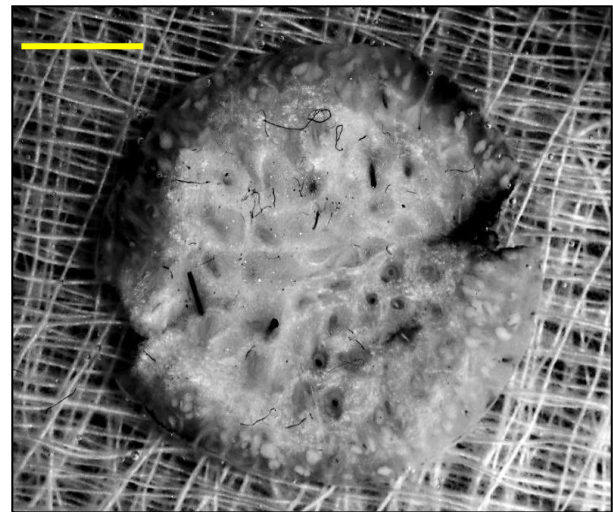


Fig. 8. Skin reflectance(cross-polarized) image at 410 nm wavelength. Exposure time was 1000 ms. Yellow bar: 3.4 mm.

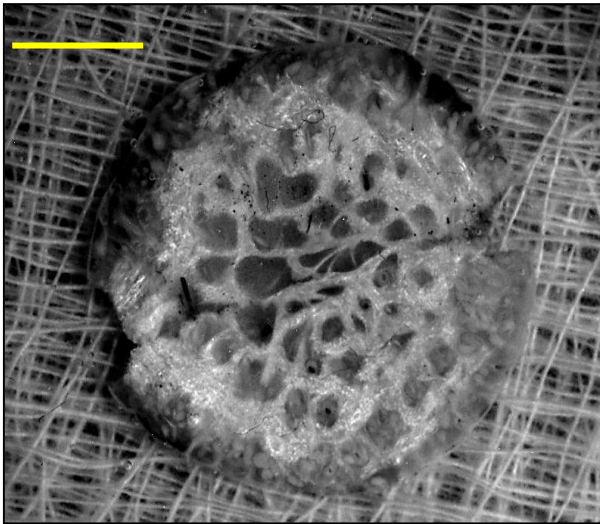


Fig. 9. Skin reflectance(cross-polarized) image at 430 nm wavelength. Exposure time was 250 ms. Yellow bar: 3.4 mm.

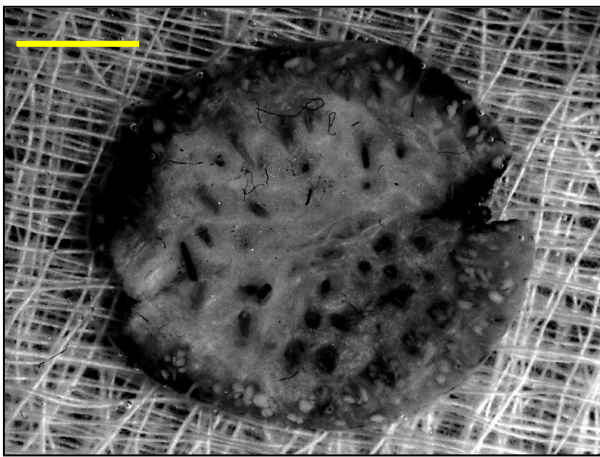


Fig. 10. Skin reflectance(co-polarized) image at 570 nm wavelength. Exposure time was 486 ms. Yellow bar: 3.4 mm.

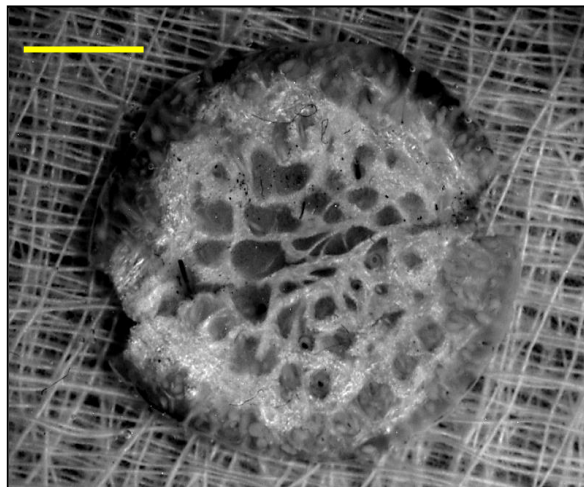


Fig. 11. Skin reflectance(co-polarized) image at 570 nm wavelength. Exposure time was 486 ms. Yellow bar: 3.4 mm.

We acquired cross and co reflectance imaged of skin tissues at different wavelengths ranging from 410 nm to 710 nm and exposure time was ranging from 250 ms to 1945 ms. The field of view shown is 20.5 mm × 15.5 mm and the bar is 3 mm.

Then we imaged breast tissues obtained from biopsies of 8 patients. The tissues were stained with methylene blue. Slides were prepared by standard protocol. For the imaging, we used 10X lens. For each slide, we took almost 200 large images that were stitched by using meta morph software as presented in figure 12 (a-d).

Our results demonstrate that there is a difference in distribution of the MB in cancerous and normal cells. Figure 12(c) demonstrates that the MB accumulates in mitochondria, lysosomes and nuclei of the cells. As cancer cells shows rapid mitosis, so region of cancer growth contains high number of nuclei as compared to normal cells. Mitochondria and lysosomes are also abundant in tumor cells. This is the reason of co-localization of MB dye in cancer cells in figure 12(a-d). Fig. 12(a) clearly demarcates a large tumor mass, as well as smaller tumor nests. Invasive ductal carcinoma is the most frequently observed type of breast cancer. The abnormal proliferation of breast ducts and infiltration of the malignant glands into the surrounding residual breast normal tissue presented in Fig 12(c). Representative sample with grade III invasive ductal carcinoma is presented in 12(d). Intra cystic papillary carcinoma is presented in Fig. 12(f). Our previous experiments show that MB being positive charge, when passes through the cell membrane, accumulates inside the mitochondria. Its accumulation level depends upon mitochondrion's membrane potential (MMP) and in breast carcinoma cells, the value of MMP is 60 mV higher than normal breast cells [24].

For spectral analysis of MB, experiments were carried out at 0.05 mg/ml and 0.01 mg/ml aqueous MB solutions. The spectrophotometer was first calibrated using 2 empty cuvettes. The absorption and emission spectrum for MB - PBS and MB - Glycerol solutions were studied in the

range of 350 - 850 nm. Absorption values were measured using arbitrary units, and then vertical axes normalized from 0 - 1, where 0 represents no absorption and 1 represents the maximum absorption.

The absorption peaks in both mixtures were observed at 664 nm. Excitation was set at 664 nm (the maximum absorption wavelength). Slit-width of 5 nm was used (figure 13).

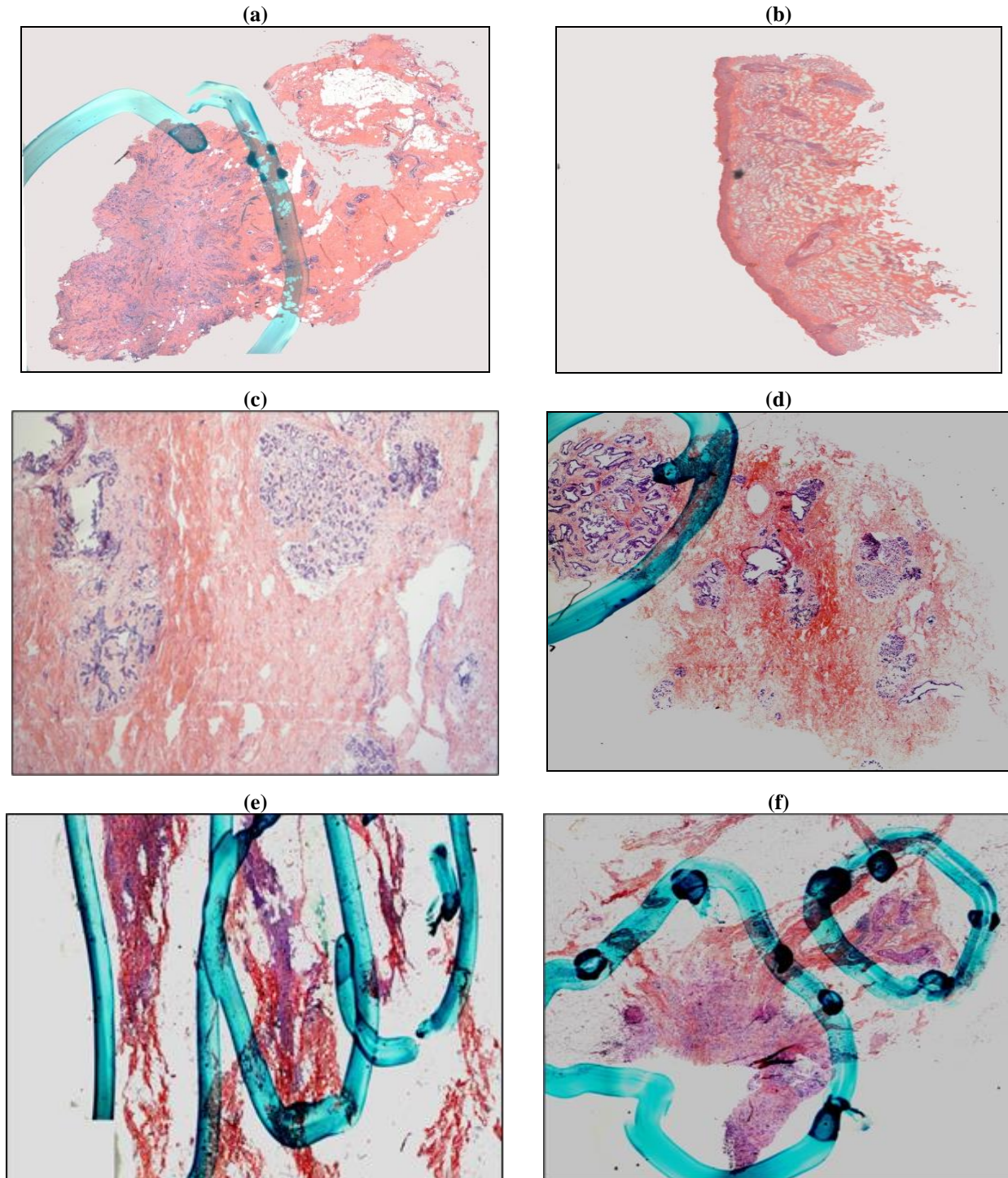


Fig. 12. H&E breast tissues stained with Methylene Blue (a-d). Different regions marked in histopathology, demonstrates smaller ducts with tumor. It also shows that although dye uptake in the tumor is higher as compared to normal tissue (e,f).

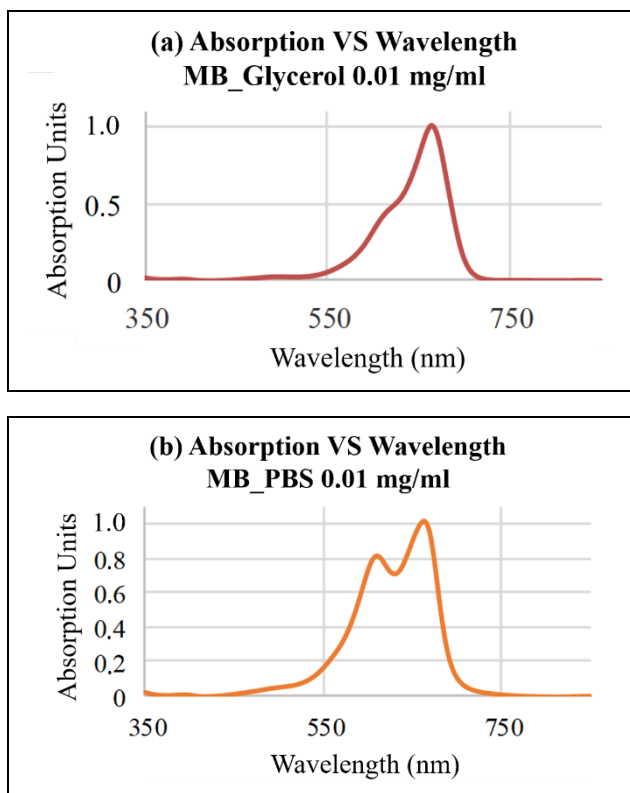


Fig. 13. (a) Absorption-vs-wavelength Graph of glycerol solution, (b) Absorption-vs-wavelength Graph of saline solution.

Then the experiment was performed for measuring the emission spectrum for MB-Glycerol and MB-Saline solution was obtained. The obtained data was plotted and represented in figure 14(a,b) below. The Graph in figure 14(a) shows emission versus wavelength of the 0.01 mg/mL MB-Glycerol solution. The emission peak occurred at 699 nm.

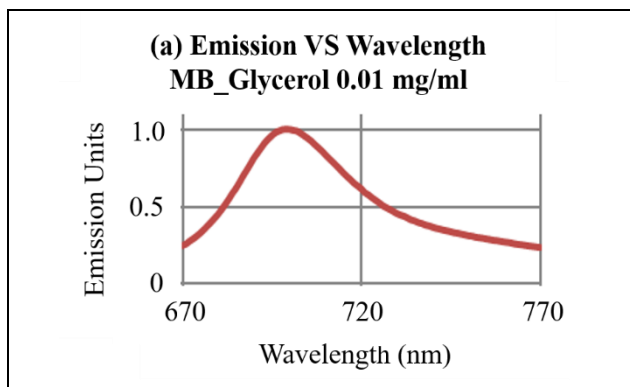


Fig. 14a. Emission-vs-wavelength Graph of Glycerol solution.

The Graph in 14(b) represents emission versus wavelength plot of the 0.01 mg/mL MB-PBS solution. The emission peak occurred at 691 nm.

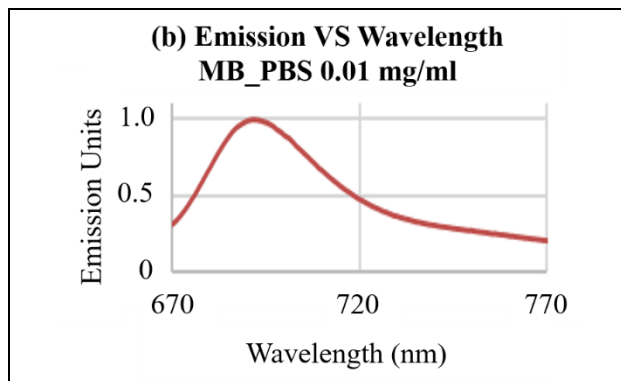


Fig. 14b. Emission-vs-wavelength Graph of saline solution.

Figure 15(a) Shows fluorescence polarization versus wavelength of the 0.01 mg/mL MB-Glycerol solution. Figure 15(b) represents fluorescence polarization versus wavelength of the 0.01 mg/mL MB-PBS solution.

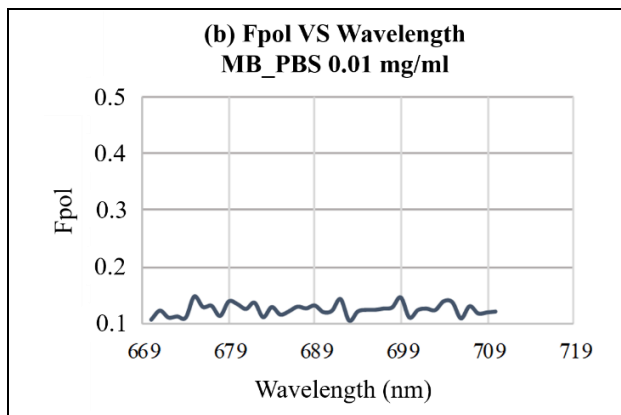
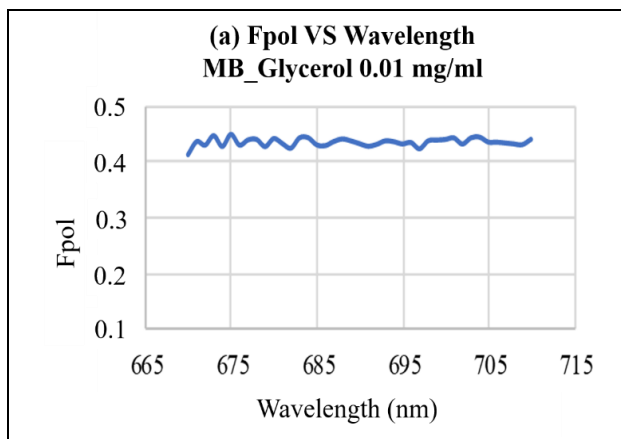


Fig. 15. (a) Fpol vs wavelength Graph of Glycerol solution and (b) Fpol vs wavelength Graph of Saline solution.

Figure 16 below reveals the combined Fpol-vs-wavelength graph of MB-Glycerol and MB-PBS solutions. The gradual change of fluorescence polarization values was observed for both solutions in figure 16.

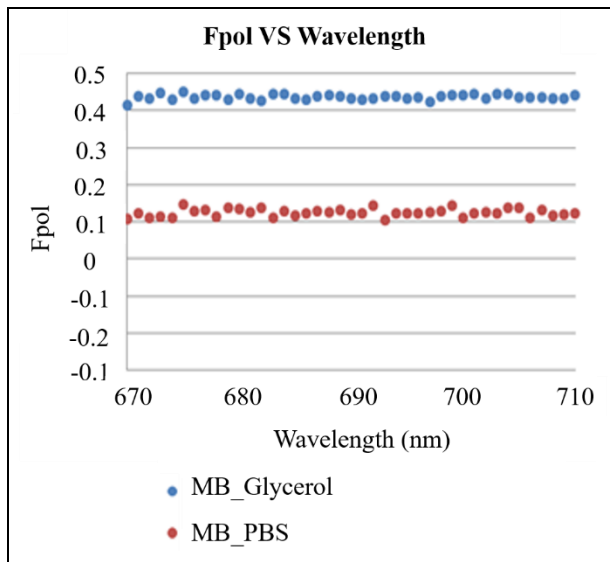


Fig.16. Fpol VS Wavelength Graph of fluorescence polarization of both solutions. Blue line represents fluorescence polarization value of MB-Glycerol solution and red line represents fluorescence polarization value of MB-PBS solution.

CONCLUSIONS

Our results indicate that MB imaging may be useful for the detection of several types of cancers [24]. It was evident that different skin features such as collagen distribution, hair glands, follicle and skin fibroids were more evident in reflectance images obtained from wide field reflectance images. We also have shown that increased MB in cancer tissue or cells can be explained by the accumulation of positively charged MB in the negatively charged mitochondria in cancer cells. In comparison to other dyes, MB has been approved by FDA and has a potential for mapping of lymph nodes. The dye can be used by surgeons in the operation room for discrimination of normal and cancerous breast cells due to high contrast thus decreasing the re-excision rates. In this experiment, we have also measured that MB-PBS and MB-Glycerol solutions both exhibit maximum absorption

of light at 664 nm. The fluorescence emission spectra of both solutions yielded an emission peak at ~690 nm, following excitation at 664 nm. Fluorescence polarization measurements indicated that the interaction mechanism of MB with Glycerol and Saline depended on the nature of the solution. Glycerol is more viscous than saline so that the Fpol of glycerol is much higher than the saline solution. Emission intensity is highly dependent on viscosity.

It is also dependent on the size of the molecules of the solution. The observed fluorescence polarization value of MB-Glycerol was 0.4 and of MB-PBS were 0.1 arbitrary units. MB is a potential biomarker in cancer diagnosis.

ACKNOWLEDGMENTS

We gratefully acknowledge Prof. Anna Yaroslavsky at Advanced Biophotonics Laboratory, Department of Physics and Applied Physics, Lowell MA, USA for her contribution and help in this experiment.

REFERENCES

- [1] Yandrapalli S., Malik A.H., Pemmasani G., Gupta K., Harikrishnan P., et al. (2020) "Risk Factors and Outcomes During a First Acute Myocardial Infarction in Breast Cancer Survivors Compared with Females Without Breast Cancer" *Am J Med.* 133(4):444-451.
- [2] Chang S., El-Zaemey S., Heyworth J., Tang M. (2018) "DDT exposure in early childhood and female breast cancer: Evidence from an ecological study in Taiwan" *Environ Int.* 121(2):1106-1112.
- [3] Vasishta S., Ramesh S., Babu P., Ramakrishnegowda A.S. (2018) "Awareness about breast cancer and outcome of teaching on breast self examination in female degree college students" *Indian J Med Spec.* 9(2):56-59.
- [4] Ullah H., Akhtar M., Batool Z., Nazir A., Mehmood R. (2021) "Physiology and stat of blood cells and parameters under hypernatremia and liquor consumption investigated at $\lambda=630$ nm" *lasers in Engineering.* 48(4-6):263-278.

- [5] Jesus V.P.S., Raniero L., Lemes G.M., Bhattacharjee T.T., Caetano P.C., Castilho M.L. (2018) "Nanoparticles of methylene blue enhance photodynamic therapy" *Photodiagnosis Photodyn Ther.* 23:212-217.
- [6] Ullah H., Rizwan M., Nazir A., Batool Z. (2021) "Analysis of liposarcoma from biopsy and mammalian blood using microscopy at $\lambda = 630$ nm and spectrophotometer ($\lambda=190-1100$ nm)" *Lasers in Engineering.* 50(4-6):267-277.
- [7] Patel R., Khan A., Wirth D., Kamionek M., Kandil D., Quinlan R., Yaroslavsky A.N. (2012) "Multimodal optical imaging for detecting breast cancer" *J Biomed Opt.* 17(6):066008.
- [8] Tummers Q.R., Verbeek F.P., Schaafsma B.E., Boonstra M.C., van der Vorst J.R., et al. (2014) "Real-time intraoperative detection of breast cancer using near-infrared fluorescence imaging and Methylene Blue" *Eur J Surg Oncol.* 40(7):850-858.
- [9] Patel R., Khan A., Quinlan R., Yaroslavsky A.N. (2014) "Polarization-Sensitive Multimodal Imaging for Detecting Breast Cancer" *Cancer Res.* 74(17):4685-4693.
- [10] Feng X., Muzikansky A., Ross A.H., Hamblin M.R., Jermain P.R., Yaroslavsky A.N. (2019) "Multimodal quantitative imaging of brain cancer in cultured cells" *Biomed Opt Express.* 10(8):4237-4248.
- [11] Patel R., Khan A., Wirth D., Kamionek M., Kandil D., Quinlan R., Yaroslavsky A. (2012) "Multimodal optical imaging for detecting breast cancer" *J Biomed Opt.* 17(6):066008.
- [12] Gordon R. (2013) "Skin Cancer: An Overview of Epidemiology and Risk Factors" *Semin Oncol Nurs.* 29(3):160-169.
- [13] Yaroslavsky A., Salomatina E., Neel V., Anderson R., Flotte T. (2007) "Fluorescence polarization of tetracycline derivatives as a technique for mapping nonmelanoma skin cancers" *J Biomed Opt.* 12(1):014005.
- [14] Yaroslavsky A.N., Patel R., Salomatina E., Li C., Lin C., Al-Arashi M., Neel V. (2012) "High-contrast mapping of basal cell carcinomas" *Opt Lett.* 37(4):644-646.
- [15] Wirth D., Snuderl M., Curry W., Yaroslavsky A. (2014) "Comparative evaluation of methylene blue and demeclocycline for enhancing optical contrast of gliomas in optical images" *J Biomed Opt.* 19(9):90504.
- [16] Yaroslavsky A., Barbosa J., Neel V., DiMarzio C., Anderson R. (2005) "Combining multispectral polarized light imaging and confocal microscopy for localization of nonmelanoma skin cancer" *J Biomed Opt.* 10(1):014011.
- [17] Yaroslavsky A.N., Feng X., Yu S.H., Jermain P.R., Iorizzo T.W., Neel V.A. (2020) "Dual-Wavelength Optical Polarization Imaging for Detecting Skin Cancer Margins" *J Invest Dermatol.* 140(10):1994-2000.e1.
- [18] Zhao Z., Wei L., Cao M., Lu M. (2019) "A smartphone-based system for fluorescence polarization assays" *Biosens Bioelectron.* 1(128):91-96.
- [19] Tranter, G.E. (2017) "Fluorescence Polarization and Anisotropy" *Encyclopedia of Spectroscopy and Spectrometry (Third Edition)*, Academic Press, pp. 632-634.
- [20] Chen J., Liu J., Chen X., Qiu H. (2019) "Recent progress in nanomaterial-enhanced fluorescence polarization/anisotropy sensors" *Chinese Chemical Letters.* 30(9):1575-1580.
- [21] Lea W.A., Simeonov A. (2011) "Fluorescence polarization assays in small molecule screening" *Expert Opin Drug Discov.* 6(1):17-32.
- [22] Malik S., Jermain P., Feng X., Yaroslavsky A. (2019) "Multimodal optical imaging of renal cells" *Optical Engineering.* 58(8):082415.
- [23] Malik S., Andleeb F., Ullah H. (2020) "Multimodal imaging of skin lesions by using methylene blue as cancer biomarker" *Microscopy Research and Technique.* 83(12):1594-1603.
- [24] Yaroslavsky A.N., Feng X., Muzikansky A., Hamblin M.R. (2019) "Fluorescence Polarization of Methylene Blue as a Quantitative Marker of Breast Cancer at the Cellular Level" *Sci Rep.* 9(1):940.